Spatiotemporal dynamics of Bose-Einstein condensates in linear- and circular-chain optical lattices

N. Tsukada*
Department of Electronics and Information Engineering, Aomori University, 2-3-1 Kobata, Aomori 030, Japan and Core Research for Evolutional Science and Technology (CREST), Japan Science and Technology (JST) Corporation, Kawaguti, Saitama 332-0012, Japan
(Received 2 January 2002; published 5 June 2002)

We investigate the spatiotemporal dynamics of Bose-Einstein condensates in optical lattices that have a linear-or a circular-chain configuration with the tunneling couplings between nearest-neighbor lattice sites. A discrete nonlinear Schrödinger equation has been solved for various initial conditions and for a definite range of repulsive and attractive interatomic interactions. It is shown that the diversity of the spatiotemporal dynamics of the atomic population distribution such as a macroscopic self-trapping, bright and dark solitons, and symmetry breaking is derived from the positive and negative interatomic interactions. For the circular-chain configuration, two types of rotational modes are obtained as we introduce a definite relation for the initial phase conditions.

DOI: 10.1103/PhysRevA.65.063608 PACS number(s): 03.75.Fi, 32.80.Pj, 42.50.Vk, 42.65.−k

The realization of Bose-Einsten condensation (BEC) in weakly interacting atomic vapors has opened the possibility to investigate nonlinear properties of atomic matter waves. Among the many features due to nonlinearities, the emergence of solitons and breathers is one of the most interesting. Intense theoretical research has now been focused on the existence of solitons and breathers in nonlinear quantum systems governed by a discrete nonlinear Schrödinger equation (DNLSE) [1].

The discrete solitons/breathers are characterized by a dynamical, self-maintained energy localization, due to both the discreteness and the nonlinearity of the underlying equation of motion. Bright solitons can occur in spatially homogeneous, dilute BEC with an attractive interatomic interaction (*s*-wave scattering length $a<0$) [2,3]. Dark solitons, propagating density dips, have been predicted and experimentally observed in BEC with a repulsive interaction ($a>0$) [4]. The dynamics of a BEC trapped in a spatially periodic potential [5–6], on the other hand, can be depicted by a DNLSE. In a recent paper [7], the problem of Bloch oscillations of bright solitons was investigated in terms of a tight-binding model for BEC arrays with positive scattering length. The dynamics of localized excitations in a BEC array was investigated in the framework of the nonlinear lattice theory by Abdullaev *et al.* [8]. They showed the existence of temporarily stable ground states displaying intrinsic localized modes as well as envelope solitons. BEC in standing waves was investigated by Bronski *et al.*, [9] by investigating a new family of stationary solutions to the cubic nonlinear Schrödinger equation with an elliptic functional potential.

The aim of this paper is to show the diversity of the spatiotemporal behaviors of atomic population distributions in coupled optical lattices (BEC arrays) for various initial conditions and a definite range of interatomic interactions.

The model. The configurations of the optical lattices investigated in this paper are shown in Fig. 1. The wave function of the system can be written as a linear combination of the wave function $\psi_j(j=1,2,...,M)$ of isolated lattice site j, i.e., $\psi(t)=\Sigma_{j=1}^{M} c_j(t)\psi_j$. The evolution of the amplitude $c_j(t)$ is described by the DNSE, or Gross-Pitaevskii equation [7–14],

$$dc_j(t)/dt = -i\Omega|c_j(t)|^2 c_j(t) - i\kappa_{j-1,j}c_{j-1}(t) - i\kappa_{j,j+1}c_{j+1}(t), \quad (1)$$

where $\Omega = U_0 N/\hbar$ with the total number of atoms N and interatomic scattering pseudopotential $U_0 = 4\pi\hbar^2 a/m$, a and m are atomic scattering length and mass, and $\kappa_{n,m}$ are the coupling (tunneling) coefficients between sites n and m. The initial condition is given by $c_j(0)=\sqrt{N_j}e^{i\phi_j}$, where N_j and ϕ_j are the normalized initial number of atoms and phases at site j. The number of atoms at site j is then given by NN_j.

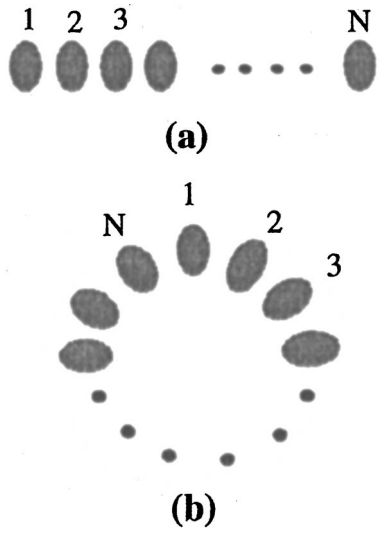

FIG. 1. Configurations of the optical lattices. (a) Linear optical lattice, (b) circular optical lattice.

*Present address: Department of Electrical and Digital-System Engineering, Hiroshima Institute of Technology, Miyake, Saeki-ku, Hiroshima, 731-5193, Japan; Email address: tsukada@cc.it-Hiroshima.ac.jp

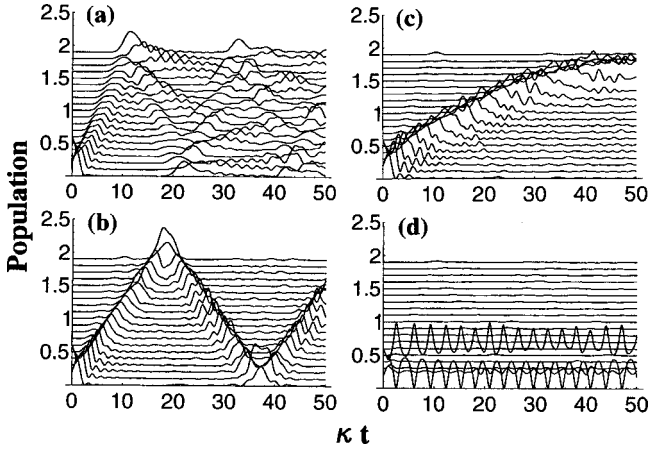

FIG. 2. The time development of the atomic populations in the linear lattice for $c_1(0)=c_2(0)=\sqrt{1/2}$ and $c_3(0)\sim c_{20}(0)=0$. (a) $\Omega/\kappa=0$, (b) $\Omega/\kappa=2$, (c) $\Omega/\kappa=3$, and (d) $\Omega/\kappa=5$. The lowest (highest) curve corresponds to site 1 (20) and the curves are successively shifted by 0.1 from site 1 to site 20.

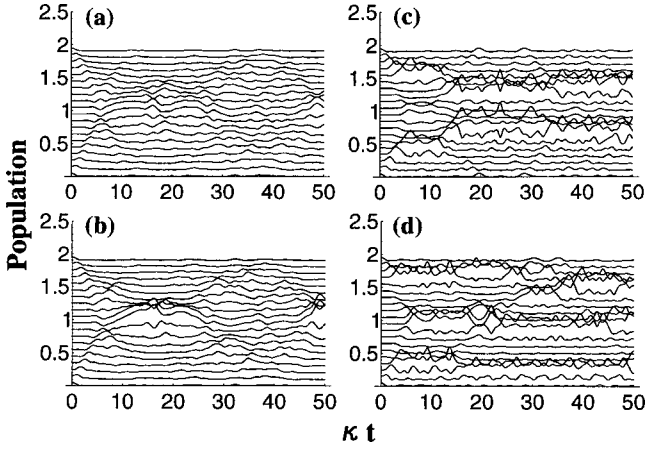

FIG. 3. The time development of the distribution of the atomic populations for $c_1(0)\sim c_{20}(0)=1/\sqrt{20}$. (a) $\Omega/\kappa=0$, (b) $\Omega/\kappa=2$, (c) $\Omega/\kappa=10$, and (d) $\Omega/\kappa=15$.

For the linear lattice with M lattice sites [Fig. 1(a)], the tunneling coupling coefficients use $\kappa_{0,1}=\kappa_{N,N+1}=0$ and $\kappa_{j,j+1}=\kappa$ (for $j=1,2,...,M-1$). While for the circular lattice [Fig. 1(b)], we should put $\kappa_{0,1}=\kappa_{N,1}=\kappa$. Throughout this paper, we consider linear and circular lattices for $M=20$ and, for almost all cases, the normalized number of atoms in the system is chosen to be one, i.e., $\Sigma_{j=1}^{20}N_j=1$.

The DNLSE [Eq. (1)] and its localized propagating modes appear in several other fields. This equation describes, for example, localized modes in molecular systems such as optical fibers and waveguides [11], long proteins [15,16], polarons in one-dimensional ionic crystals [17,18], localized modes in electrical lattices [19], arrays of Josephson junctions [20,21], a coupled array of nonlinear mechanical pendulums [22], and instabilities in one-dimensional nonlinear lattices [23].

Linear-lattice configuration. First we consider a case that one of the sites of a linear lattice [see Fig. 1(a)] is initially populated. In the absence of the nonlinear term of Eq. (1), the atoms spread into two main lobes with several secondary peaks between them [see Fig. 1 in Ref. [11], in which the length (distance) should be replaced by time]. As the nonlinearity increases, the spreading of the atomic population is suppressed since the nonlinear term compensates the spreading and eventually tends to localize on the initially populated sites. As an example, here, we show a case that two sites at one of the lattice ends are initially populated, i.e., $c_1(0)=c_2(0)=\sqrt{1/2}$ and $c_3(0)\sim c_{20}(0)=0$. In Fig. 2 we show the time development of the distribution of the atomic populations as a function of the dimensionless time κt. Each curve corresponds to the normalized population of each site. The lowest (highest) curve corresponds to site 1 (20) and the curves are successively shifted by 0.1 from site 1 to site 20. In the absence of the interatomic interactions ($\Omega/\kappa=0$), the atoms initially populated at one of the lattice edges propagate to opposite side of the lattice and then reflect at the lattice boundary, showing splitting and broadening of the wave packet [Fig. 2(a)]. For $\Omega/\kappa=2$, the wave packet maintains its shape even after the reflections at the lattice boundaries since the positive interatomic interactions (positive nonlinearity) compensate the diffusion of the wave packet [Fig. 2(b)]. We can, therefore, call this wave packet a bright soliton. As the interatomic interaction increases, the velocity of the soliton decreases [Fig. 2(c)] and finally becomes zero [Fig. 2(d)], resulting in the localization of the atoms. Although almost all atoms localized at the initially populated two sites, the population exchange between the two sites can be seen. It should be noted that the same results are obtained for negative values of the nonlinearity ($\Omega/\kappa=-2$), if one of the phases of the initial order parameters $c_1(0)$ and $c_2(0)$ is changed by π, i.e., $c_1(0)=1/\sqrt{2}$, $c_2(0)=e^{-i\pi}/\sqrt{2}$ or $c_1(0)=e^{-i\pi}/\sqrt{2}$, $c_2(0)=1/\sqrt{2}$ [24].

Figure 3 shows the time development of the population distribution for the initial conditions with an uniform distribution of the atoms in all sites, i.e., $c_1(0)\sim c_{20}(0)=1/\sqrt{20}$. In the absence of nonlinearity ($\Omega/\kappa=0$), the population distribution shows a somewhat complex behavior. Two wave packets generated at the lattice boundaries counterpropagate and interfere destructively at the center of the lattice, resulting in the repulsion of the wave packets and successive interference in a complex manner [Fig. 3(a)]. Increasing the positive nonlinearity ($\Omega/\kappa=2$), the populations gradually converge into the central region and most part of the populations localizes on the two central sites for $10\leqslant\kappa t\leqslant 25$, and then the populations again disperse on nearly all sites for $25\leqslant\kappa t\leqslant 45$ [Fig. 3(b)]. The periodic localization and dispersion occur as a function of the time. Increasing the nonlinearity further, most atoms localize on two spatially separate regions of sites 8 and 13 [Fig. 3(c)]. The population distribution is still symmetric about the center of the lattice and hence the symmetric sites 10 and 11 have the same population. For $\Omega/\kappa=15$, spatially separated three self-trapping regions appear and the symmetry breaking, which shows the asymmetric population distributions for the symmetric sites 10 and 11, can be seen at $\kappa t\geqslant 22$ [Fig. 3(d)]. After the symmetry breaking occurs, the time development of the population distribution becomes more complex. We have confirmed that as the positive nonlinearity increases further, the local-

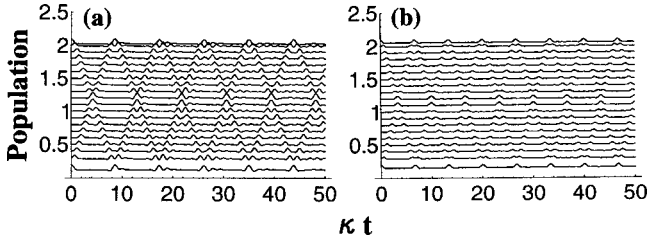

FIG. 4. The same as Fig. 3 but for the negative interatomic interactions. (a) $\Omega/\kappa=-40$ and $\Omega/\kappa=-80$. The populations are magnified four times.

ization tends to occur on equally separated sites, i.e., localization on two spatially separated regions for $\Omega/\kappa=10$, three regions for $\Omega/\kappa=15$, and four regions for $\Omega/\kappa=25$.

As the negative nonlinearity (attractive interaction) is increased, it seems at first glance that the population distribution becomes more and more homogeneous. However, if we magnify the scale of the population, the bright solitons can be clearly seen as shown in Fig. 4. The numerical results obtained for $\Omega/\kappa=-40$ and -80 are shown in Figs. 4(a) and 4(b), respectively. The vertical axis (atomic population) in Fig. 4 is magnified four times. We can see two solitons generated at the lattice boundaries, which propagate along opposite directions and encounter each other at the center of the lattice, preserving their shapes before and after the collision. They reflect at the lattice boundaries and form traces of multiple reflections making diamond patterns. The speed (amplitude) of the soliton increases (decreases) as the absolute value of Ω/κ is increased. It is verified that the velocity and amplitude are well fitted by logarithmic curves as a function of Ω/κ. The logarithms of the velocity and amplitude against the logarithm of Ω/κ exhibit straight lines. Again we stress that the same results as those shown in Fig. 4 could be obtained even for the positive (repulsive interaction) nonlinear parameters that have the same absolute values with the initial phase condition of $\phi_j=0(\pi)$ for odd sites and $\phi_j=\pi(0)$ for even sites. In practical experiments, the phase shift can be realized by means of phase imprinting [25]. This means that the negative nonlinearity is not a necessary condition to obtain the dynamical localization of the atoms and the self-trapping occurs even for the positive nonlinearity (repulsive interatomic interaction).

The dark and bright solitons can be created by changing the initial population distributions. For example, the creation of the solitons for different values of the populations at two sites of the lattice edges is shown in Fig. 5. The amplitude of the populations is magnified four times. We assume that the populations of the rest sites are homogeneous, i.e., $c_2(0)\sim c_{19}(0)=1/\sqrt{20}$ and $\Omega/\kappa=-50$. When the populations of the edge sites is reduced to be less than those of other sites, say $c_1(0)=c_{20}(0)=0.2/\sqrt{20}$, apparent dark solitons appear as shown in Fig. 5(a). For $c_1(0)=c_{20}(0)=0.8/\sqrt{20}$, the soliton becomes very obscure with a shallow depth [Fig. 5(b)]. The velocity of the dark solitons decreases as the edge population is reduced. In Figs. 5(c) and 5(d), we show the bright solitons obtained for $c_1(0)=1.2/\sqrt{20}$ or $1.5/\sqrt{20}$. The velocity as well as the amplitude of the bright solitons increases as the edge populations are increased.

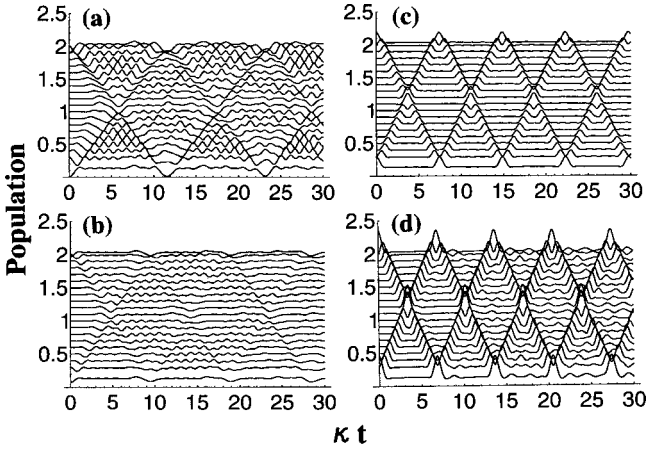

FIG. 5. The dark and bright solitons obtained for different values of the populations at two sites of the lattice ends with $c_2(0)\sim c_{19}(0)=1/\sqrt{20}$ and $\Omega/\kappa=-50$. (a) $c_1(0)=c_{20}(0)=0.2/\sqrt{20}$, (b) $c_1(0)=c_{20}(0)=0.6/\sqrt{20}$, (c) $c_1(0)=1.2/\sqrt{20}$, and (d) $c_1(0)=1.5/\sqrt{20}$.

Circular-lattice configuration. Here we consider the time development of the population in a circular lattice [see Fig. 1(b)] for the initial conditions with uniform distribution of the atoms in the system, i.e., $c_1(0)\sim c_{20}(0)=1/\sqrt{20}$ [10]. In the absence of the nonlinear term, i.e., $\Omega/\kappa=0$, no change of the population distribution occurs since all sites have the same symmetry. Upon increasing the positive nonlinearity, the very small population fluctuation induces symmetry breaking of the population distribution and, consequently, the large parts of the populations initially distributed in all sites tend to localize on one or two sites. If the population fluctuation of one of the sites is positive (negative), the large part of the populations tends to localize on that (opposite or symmetric) site. The numerical result introduced the positive population fluctuation at site 10, i.e., $c_{10}(0)=1.0001/\sqrt{20}$, is shown in Figs. 6 for various values of the nonlinearity. For relatively small values of the nonlinearity, the atoms tend to localize on around site 10. For large nonlinearities, the atoms

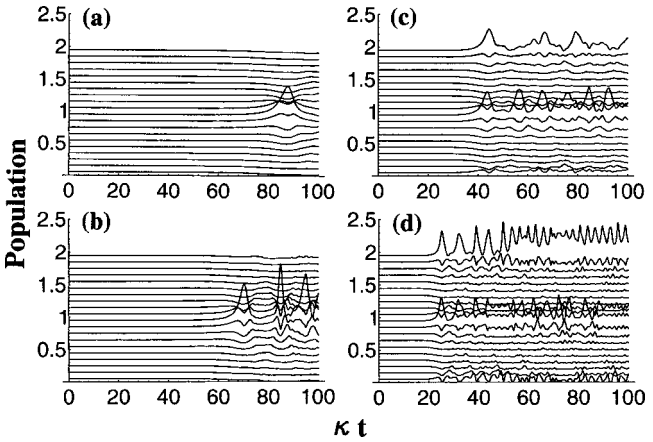

FIG. 6. The time development of the atomic populations in the circular lattice for $c_{10}(0)=1.0001/\sqrt{20}$ and $c_1(0)\sim c_9(0)=c_{11}(0)\sim c_{20}(0)=1/\sqrt{20}$. (a) $\Omega/\kappa=3$, (b) $\Omega/\kappa=4$, (c) $\Omega/\kappa=6$, and (d) $\Omega/\kappa=10$.

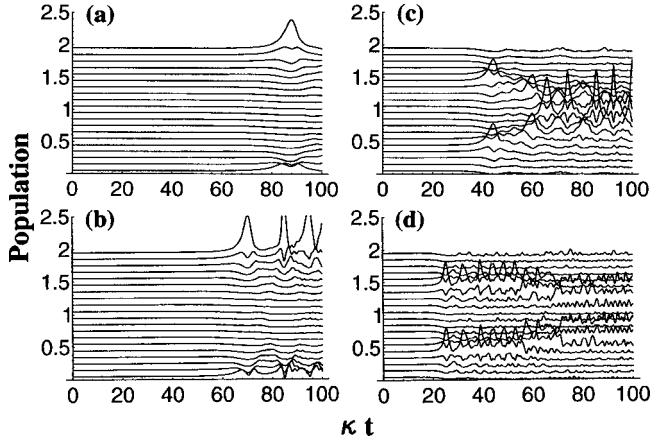

FIG. 7. The same as Fig. 6 but for $c_{10}(0)=0.9999/\sqrt{20}$. (a) $\Omega/\kappa=3$, (b) $\Omega/\kappa=4$, (c) $\Omega/\kappa=6$, and (d) $\Omega/\kappa=10$.

tend to localize on two regions, site 10 and its symmetric site 20. On the other hand, the results for negative population fluctuation at site 10, i.e., $c_{10}(0)=0.9999/\sqrt{20}$, is shown in Fig. 7. For relatively small values of the nonlinearity, the atoms tend to mainly localize on site 20. As the nonlinearity increases, the atoms tend to localize on two regions, i.e., sites 5 and 15. From a practical point of view, it seems important to note that the addition or subtraction of a very small number of atoms to or from one of the sites induces the symmetry breaking of the atomic population distributions, which results in the abrupt localization of the large part of atoms on one of the sites [10].

No symmetry breaking can be seen for the negative interatomic interactions and the homogeneous population distribution is maintained even for infinitely large nonlinearities. If one or two sites have larger or smaller populations compared to other sites' populations that give nonzero background populations, the bright or dark solitons are created for the negative nonlinearity. The bright solitons obtained for the initial conditions $c_{10}(0)=3/\sqrt{20}$ and $c_1(0)\sim c_9(0)=c_{11}(0)\sim c_{20}(0)=1/\sqrt{20}$ with $\Omega/\kappa=-5$ are shown in Fig. 8(a). The dark solitons obtained for $c_{10}(0)=c_{11}(0)=0.5/\sqrt{20}$ and $c_1(0)\sim c_9(0)=c_{12}(0)\sim c_{20}(0)=1/\sqrt{20}$ with $\Omega/\kappa=-35$ are shown in Fig. 8(b) in which the amplitude of the populations is magnified four times. Both bright and dark

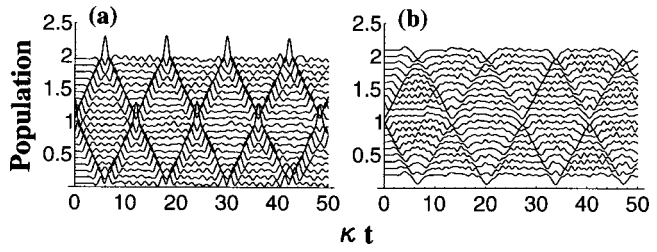

FIG. 8. (a) The bright solitons obtained for the initial conditions $c_{10}(0)=3/\sqrt{20}$ and $c_1(0)\sim c_9(0)=c_{11}(0)\sim c_{20}(0)=1/\sqrt{20}$ with $\Omega/\kappa=-5$. (b) The dark solitons obtained for $c_{10}(0)=c_{11}(0)=0.5/\sqrt{20}$ and $c_1(0)\sim c_9(0)=c_{12}(0)\sim c_{20}(0)=1/\sqrt{20}$ with $\Omega/\kappa=-35$.

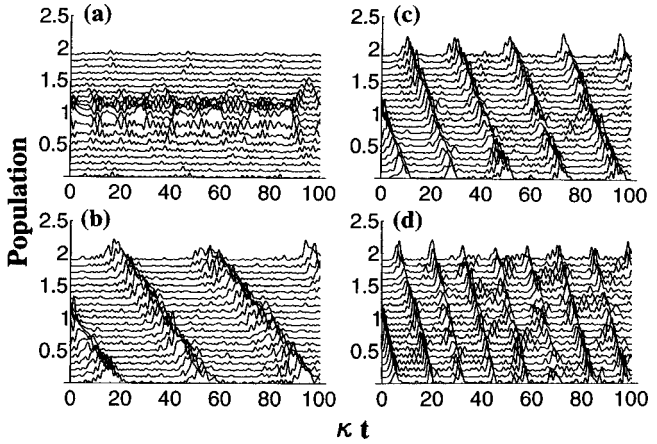

FIG. 9. The rotational solitons obtained for the initial conditions of $c_9(0)=1/2$, $c_{10}(0)=e^{i\varphi}/2$, $c_{11}(0)=e^{i2\varphi}/2$, $c_{12}(0)=e^{i3\varphi}/2$, and for the nonlinearity of $\Omega/\kappa=2.5$. (a) $\varphi=0$, (b) $\varphi=0.1\pi$, (c) $\varphi=0.2\pi$, and (d) $\varphi=0.4\pi$.

solitons contain two counterrotating components with an equal amplitude or depth.

Considering the population dynamics in circular lattice configuration, it is quite natural to consider the rotation of the atomic populations in the system. In order to rotate the atoms we introduce a definite phase relation into the initial conditions. Figure 9 shows one of such results obtained for the initial conditions of $c_9(0)=1/2$, $c_{10}(0)=e^{i\varphi}/2$, $c_{11}(0)=e^{i2\varphi}/2$, and $c_{12}(0)=e^{i3\varphi}/2$, and for the nonlinearity of $\Omega/\kappa=2.5$. If the phase parameter φ is zero, the large part of the populations localizes initially populated four sites [Fig. 9(a)]. Introducing the nonzero phase parameters, the atoms can move from site to site resulting in the rotational solitons in the circular lattice. The velocity of the population rotation depends on values of the phase parameter. Upon increasing the phase φ, the rotational velocity becomes larger [Figs. 9(b)–9(d)]. It seems that the velocity is nearly proportional to the phase φ within its small values but seems to be saturated for large values. This is the reason why the highest velocity of the rotational soliton is limited by the bare tunneling coefficient κ. The velocity cannot exceed the transfer time determined by the bare tunneling coefficient κ and therefore the rotational solitons become gradually irregular and eventually disappear as the value of φ is increased. If we change the sign of the phase shift $\varphi\rightarrow-\varphi$, the direction of rotation is reversed.

The effect of the nonlinearity on the velocity of the rotational solitons is investigated. It is clear that the rotational velocity decreases as the nonlinearity is increased. The rotational solitons are observed only for a definite positive values of the nonlinearity. Outside of this parameter space, the rotational solitons become intermittent and finally disappear.

There is another type of rotational transfer mode of the atoms, which is obtained for the initial conditions with uniform population distribution and the phases proportional to the number of sites. Such a rotational mode is obtained for $c_n(0)=e^{in\varphi}/\sqrt{20}$ $(n=1,2,...,20)$.

Figure 10 shows the numerical results for $\Omega/\kappa=1.0$ and for different values of the phase parameter φ. When the ac-

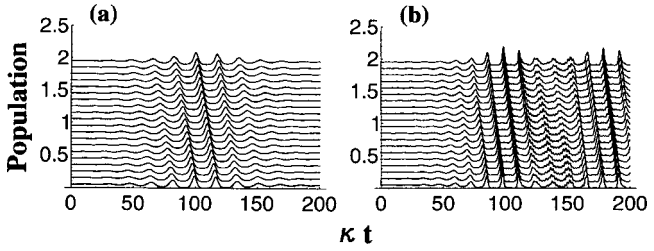

FIG. 10. The rotational mode obtained for $c_n(0)=e^{in\varphi}/\sqrt{20}$ ($n=1,2,...,20$) and $\Omega/\kappa=1.0$. (a) $\varphi=0.199\pi$ and (b) 0.299π.

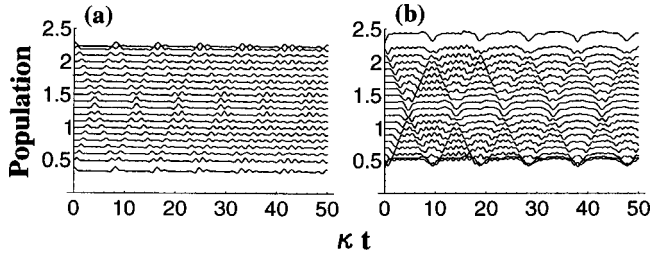

FIG. 11. The bright and dark solitons induced by the defects of lattices for $c_1(0)\sim c_{20}(0)=1/\sqrt{20}$ and $\Omega/\kappa=-50$, (a) $\kappa_{1.20}=\kappa_{20.1}=0.5\kappa$ and (b) $\kappa_{1.20}=\kappa_{20.1}=2\kappa$. The populations are magnified eight times.

cumulated one-round phase, which is given by multiplication of phase parameter φ and the number of lattice sites ($M=20$), becomes $2m\pi$ ($m=0,1,2,...$), there is no population change and the population distribution appears homogeneous. The clear rotational modes can be seen for the values of $\varphi=0.199\pi$ [Fig. 10(a)] and $0.299\ \pi$ [Fig. 10(b)], which are a little bit smaller than $\varphi=2m\pi$ ($m=0,1,2,...$). These clear rotational modes cannot be obtained in the absence of the positive nonlinearity. The periodic growth and extinction of the rotational wave packets are clearly seen in Fig. 10. There is a time delay before the start of growth in the rotational wave packet. Alike the rotational solitons shown in Fig. 9, the velocity of the rotational wave packet is nearly proportional to the phase shift φ.

We investigate the effects of the nonlinearity on the rotational mode for a constant phase parameter φ. In the absence of interactions ($\Omega/\kappa=0$), faint rotational waves are seen. Increasing the interactions, the rotational waves become clearer and show the periodic growth and extinction. The period between the growth and extinction becomes short as the interaction is increased. In contrast to the previous rotational mode, the rotational velocity is nearly constant, regardless of the values of the interactions and is determined only by the values of the phase parameter φ.

Defects in the lattices. We study the effects of the defects on the dynamics of the time development of the populations by introducing the defects in the lattices, which are imitated by a site with different values of coupling (tunneling) coefficient κ and/or nonlinearities Ω/κ from those of other sites. Figure 11 shows the results by introducing a variable coupling coefficient between site 1 and site 20, i.e., $\kappa_{1,20}$ or $\kappa_{20,1}$, in the circular lattice configuration. The initial conditions are $c_1(0)\sim c_{20}(0)=1/\sqrt{20}$ and $\Omega/\kappa=-50$. If $\kappa_{1,20}=\kappa_{20,1}=0$, the system becomes equivalent to a linear lattice and again the bright solitons produced from the lattice boundaries are seen. Increasing the coupling coefficient $\kappa_{1,20}=\kappa_{20,1}$ from 0 to κ, the amplitude of the bright solitons becomes smaller and smaller [see Fig. 11(a) for $\kappa_{1,20}=\kappa_{20,1}=0.5\ \kappa$] and eventually disappears at $\kappa_{1,20}=\kappa_{20,1}=1$, which corresponds to the circular lattice without the defect. Increasing the coupling coefficient beyond κ, the dark soliton grows up until $\kappa_{1,20}=\kappa_{20,1}=4\ \kappa$ [see Fig. 11(b) for $\kappa_{1,20}=\kappa_{20,1}=2\ \kappa$], beyond this value the dark soliton gradually diffuses in a complex manner. Further increasing $\kappa_{1,20}=\kappa_{20,1}$, the two edge sites have large populations because of the nonresonant level formation by the strong coupling. The strong coupling between site 1 and site 20 induces a large level splitting of symmetric and antisymmetric states. This makes a sharp boundary and, consequently, the bright solitons appear again. Similar results are obtained by introducing different values of the nonlinearity Ω/κ at one of the sites.

Discussion and conclusions. We investigate the spatiotemporal dynamics of BEC in optical lattices that have a linear or a circular configuration with tunneling couplings between nearest-neighbor lattice sites. The coupled nonlinear Schrödinger equation has been solved with various initial conditions and with positive and negative nonlinearities. The diversity of the spatiotemporal dynamics for the population distributions such as a macroscopic self-trapping, bright and dark solitons, and symmetry breaking is shown to be derived from the positive and negative interatomic interactions. For the circular-chain configuration, if we introduce the appropriate initial phase conditions, two kind of the rotational modes were predicted. Furthermore, we have considered the effect of the lattice defects imitated by a site with different values of the coupling coefficient and/or the interatomic interactions and shown the appearance of bright and dark solitons induced by the lattice defects.

This work is partially supported by a Grant-in-Aid from the Ministry of Education, Science, Sports and Culture (Grant No. 20275514).

[1] See, e.g., Physica (Amsterdam) **68D**, 1 (1993), special issue on future directions of nonlinear dynamics in physics and biological systems, edited by P. L. Christiansen, J. C. Eilbeck, and P. D. Parmentier.
[2] D. Jaksh *et al.*, Phys. Rev. Lett. **81**, 3108 (1998).
[3] O. Zobay *et al.*, Phys. Rev. Lett. **82**, 3288 (1999).
[4] S. Burger *et al.*, Phys. Rev. Lett. **83**, 5198 (1999).
[5] K. B. Sorensen and K. Molmer, Phys. Rev. A **58**, 1480 (1999).
[6] J. Javanainen, Phys. Rev. A **60**, 4902 (1999).
[7] A. Trombettoni and A. Smerzi, Phys. Rev. Lett. **86**, 2353 (2001).
[8] F. Kh. Abdullaev, B. B. Baizakov, S. A. Darmanyan, V. V.

Konotop, and M. Salerno, Phys. Rev. A **64**, 043606 (2001).
[9] J. C. Bronski, L. D. Carr, B. Deconinck, and J. N. Kutz, Phys. Rev. Lett. **86**, 1402 (2001).
[10] N. Tsukada, M. Gotoda, T. Isu, M. Nunoshita, and T. Nishino, Jpn. J. Appl. Phys., Part 2 **36**, L834 (1997).
[11] H. S. Eisenberg, Y. Silberberg, R. Moramdotti, A. R. Boyd, and J. S. Aichison, Phys. Rev. Lett. **81**, 3383 (1998).
[12] D. Hennig and G. P. Tsironis, Phys. Rep. **307**, 333 (1999).
[13] K. O. Rasmussen, T. Cretwgny, P. G. Kevrekidis, and N. G. Gronbech-Jensen, Phys. Rev. Lett. **84**, 3740 (2000).
[14] P. G. Kevrekidis, K. O. Rasmussen, and A. R. Bishop, Phys. Rev. E **61**, 4652 (2000).
[15] A. V. Vavydov, Phys. Scr. **20**, 387 (1978).
[16] M. Peyrard *et al.*, Physica (Amsterdam) **68D**, 104 (1993).
[17] J. D. Andersen and V. M. Kenkre, Phys. Rev. B **47**, 11 134 (1993).
[18] T. Holstein, Mol. Cryst. Liq. Cryst. **77**, 235 (1981).
[19] P. Marquie, J. M. Bilbault, and M. Romoissenet, Phys. Rev. E **51**, 6127 (1995).
[20] E. Trias, J. J. Mazo, and T. P. Orlando, Phys. Rev. Lett. **84**, 741 (2000).
[21] P. Binder *et al.*, Phys. Rev. Lett. **84**, 745 (2000).
[22] B. Denardo *et al.*, Phys. Rev. Lett. **68**, 1730 (1992).
[23] A. M. Morgante, M. Johansson, G. Kopidakis, and S. Aubry, Phys. Rev. Lett. **85**, 550 (2000).
[24] In two coupled well system, it was shown by use of the Bloch sphere that changing one of the initial phase by π is equivalent to changing the sign of the nonlinearity: N. Tsukada, Phys. Rev. A **64**, 033601 (2001).
[25] S. Burger *et al.*, Phys. Rev. Lett. **83**, 5198 (1999).